Smart Agricultural Technology 2 (2022) 100056

Contents lists available at ScienceDirect

Smart Agricultural Technology

journal homepage: www.elsevier.com/locate/atech

# Automatic detection of insect predation through the segmentation of damaged leaves

Gabriel da Silva Vieira [a,b], Bruno Moraes Rocha [b], Afonso Ueslei Fonseca [b], Naiane Maria de Sousa [b], Julio Cesar Ferreira [a], Christian Dias Cabacinha [c], Fabrizzio Soares [b,*]

[a] Federal Institute Goiano/IFGoiano, Computer Vision Laboratory, Urutaí - GO, Brazil
[b] Federal University of Goiás/UFG, Institute of Informatics, Goiânia - GO, Brazil
[c] Federal University of Minas Gerais/UFMG, Institute of Agrarian Science, Montes Claros - MG, Brazil

ARTICLE INFO

*Keywords:*
Leaf segmentation
Foliar analysis
Insect predating
Smart farming
Precision agriculture

ABSTRACT

Leveraged by the production of grains, oilseeds, and fresh deciduous fruits, food production has reached new heights, exceeding the amount produced in previous years and with an estimate of new records for the coming years. In this sense, technological advances are essential to reduce costs and increase quality and productivity. In this paper, we present a novel method to detect insect predation on plant leaves that uses geometric leaf properties and digital image processing techniques to construct image models. Unlike other approaches, our method detects and highlights the regions of leaves attacked by insects and segments the contours of insect bites. We evaluated our proposal considering 12 crucial crops for the world market, and it demonstrated to be effective, even in the presence of noise, image scale, and rotation. Besides, it identifies insect predation areas regardless of the plant species with precision above 90% in blueberry, corn, potato, and soybean leaves. Thus, this proposal introduces a new approach to automatic leaf analysis and contributes to reducing human effort in identifying the occurrence of pests. The code prepared by the authors is publicly available.

## 1. Introduction

The activities performed in agricultural fields respond to high value-added businesses, being economically important in the production of grains, oilseeds, ornamental and medicinal plants, and green vegetables. World soybean production reached 336.59 million metric tons (Mmt) in 2019/2020, moving 31.2 billion U.S. dollars, with only the United States production of 96.67 Mmt [1]. Although lower than the production of 2018/2019, Corn production reached 1,116.2 Mmt, with an average price of around $362 per ton, the highest since August 2015 [2]. Centrifugal sugar production reached 166.17 Mmt in which Brazil has been leading the world production in the last five years with production above 29.92 Mmt [3].

In the same way, fresh deciduous fruits and stone fruits play an important role in global food production. In 2020, China was the largest producer of apples, grapes, and pears, launching more than 62 million tons of these fruits in the domestic consumer market [4]. Furthermore, in that same year, the European Union and Chile exported the most significant number of peaches and cherries, in a total of 395 metric tons [5].

The improvement of technologies for automation contributes significantly to agricultural production, making it more effective and sustainable through intelligent support for decision making, operation, and agricultural management [6]. Methods for detecting leaf damage and monitoring insects in crop fields are examples of computer vision and machine learning techniques to address real problems that can cause significant losses in the production process. Therefore, if an attack of insects is detected in advance, the management of solutions can be more accurate, saving resources and safeguarding cultivation, potentially increasing yield, and protecting crops.

The detection of insects allows the analyst to verify occurrences of losses above expectations and carry out mitigation and control actions. This verification is necessary to distinguish between situations of normality in which the ecosystem is in balance and when the population growth of certain species becomes a risk factor for agricultural development. Because of this, some proposals focus on insect detection and classification through computer learning systems where several samples of insect images are collected to build classification models using machine learning algorithms [7–9].

Although detection systems make it possible to identify the presence of insects in plantations, it is difficult to infer from them the line that crosses population normality and the outbreak of a given species. Among the factors that limit these solutions, the mobility of insects between plants stands out because as they move, there may be different records

* Corresponding author.
*E-mail address:* fabrizzio@inf.ufg.br (F. Soares).

https://doi.org/10.1016/j.atech.2022.100056
Received 14 February 2022; Received in revised form 9 April 2022; Accepted 10 April 2022

for the same specimen in different plants, and vision systems may not be able to record their presence when they move fast or are camouflaged, hidden and in clusters. On the other hand, damage caused by insects is limited to the location of the injured plants, which can be used to direct foliar analyzes and verify the local and global health of the crops, even in the absence of the insect that induced the losses. From there, inferences about the ecological balance can be made.

In this sense, we propose a novel approach to identifying insect predation marks and point out the places where leaf damage occurs. Therefore, we do not detect insects but the damage caused by them. It is a way of treating the same problem in an innovative way to identify the occurrence of insects in the plantation even with their absence. Thus, it makes our method more versatile as it can detect damage of different proportions, including damage to leaf border regions and pest incidence at different stages of development.

Quantifying the number of damaged leaves is a potential use of the proposed method that can answer questions related to insect population growth, the ability of plants to develop in the face of predators, and whether there is a potential risk to crop fields. In these cases, the previous analysis would justify the conduction of interventions to reduce losses and re-balance the ecosystem in the crops. Furthermore, the bite trace segments presented as an output of the proposed method enable the analyst/specialist through visual inspection to determine the category of insects, for example, differentiating leaf-chewing insects (e.g., caterpillars) from leaf-cutting insects (ants, leafcutter bees, grasshopper, and others).

Our method uses geometric leaf properties and digital image processing techniques to construct image models. Initially, healthy leaves are used as input in the model construction process. Then, with the constructed models, an injured leaf is processed, and the image model that best fits it is selected and used to detect the damaged leaf areas and segment the insect bites. The strategies used in this proposal demonstrated to be effective in the presence of noise and geometric distortions caused by image acquisition processes, in the detection of insect predation in different foliar structures, and morphologies, and in the segmentation of insect bites in low or severe defoliation.

We evaluated our proposal considering 12 critical crops for the world market, including soybean, sugarcane, corn, apple, grape, peach, and cherry. We explore different levels of defoliation in a vast and diverse set of leaf images and investigate the behavior of our method in computer vision challenges, such as image rotation, scale variation, and noise. Due to the assertiveness of the proposed method, the results are promising to assist experts, agronomists, ecophysiologists, and farmers in making better decisions in cultivars, including insecticide evaluations and proper crop management.

The main contributions of the proposed method are:

- A novel method for recognition of insect attack on planting leaves.
- A systematic approach to highlighting insect-damaged leaf regions.
- A synthetic defoliation strategy using real insect attack cases.
- A methodology for evaluating line segmentation approaches (insect bite traces).

The remainder of the paper is organized as follows. Section 2 summarizes existing studies of insect predation in crop fields. Section 3 introduces our proposed method in detail. Section 4 describes vital information about the experimental design, such as the database used and evaluation metrics. Section 5 provides the experimental results and analysis. Section 6 presents a discussion of the results. Finally, the work done is concluded in Section 7.

## 2. Related work

Several works use digital image processing and machine learning algorithms to identify pests in different crop fields. Wang et al. [10], for example, classified insects using digital images in which a manual processing approach was performed to remove the background and highlight only the insect region. Thus, feature extraction was applied to the insect images previously segmented to obtain information about the body radius, body shape parameter, color complexity, head size, and thorax of the insects. Then, the acquired information was indexed to classify the insects using Support Vector Machines (SVM).

Similarly, Wen and Guyer [11] presented an automatic method for identifying insects in digital images using local and global features. The Scale Invariant Feature Transform (SIFT) was used to identify local features and record them into a histogram. Also, a color-based clustering segmentation method was applied to obtain global information as the shape and contour of the insect. The K-means cluster separated the insect area from the background and the insect shape, texture, and colors corresponding to 54 global features and 100 local features for each image. These local and global features were used to categorize the images using five different classifiers (Minimum Least Square Linear, Normal Densities Base Linear, K-Nearest Neighbor Classifier, Nearest Mean, and Decision Tree).

Xie et al. [12] also used the descriptors of color characteristics (color histogram), texture, shape (United Moment-Invariant), SIFT, and Histogram of Oriented Gradients (HOG) to obtain image features. The SVM classifier labeled the images using Multiple Kernel Learning (MKL). In the same way, Yang et al. [13] developed a system to detect owlfly insects based on the contours of their wings. In this proposal, the image background was manually removed using graphic editing software, and the image was transformed into a grayscale and binarized to separate the contours of the insect's wings. Furthermore, the C-Support Vector Classification algorithm was used to classify the images.

Thenmozhi and Reddy [14] presented a method to detect the presence of insects in sugarcane crops. Initially, RGB images were converted to grayscale, and the images were divided into smaller regions to determine the edges or boundaries using Canny, Sobel, Gaussian HPF, and Prewitt Edge detection filters. Then, the feature extraction strategy was performed using boundary form, surface, and textures of insects, and the classification was performed to evaluate the similarity of the body of insects concerning some geometric shapes such as triangles, circles, and rectangles.

In Deng et al. [15], the detection of insect pests was based on the human visual system in which the FastICA Efficient Projection Map was used to detect the region of interest (ROI). Then, the processed images were normalized, and the Otsu method was applied to find the threshold that could better define the ROI. Next, Gabor Filters were applied to detect edges, and the SIFT and Local Binary Pattern were used to extract gradient and texture orientation features, respectively. Finally, SVM with a radial basis function was used to classify the images.

Another technique widely used to classify objects is deep learning. In Cheng et al. [16], multiple layers of abstraction, called ResNet-101, were used to classify insects in digital images. Shen et al. [17] used the Faster R-Convolutional Neural Networks (R-CNN) to segment insects in grain and classify them. Likewise, Kasinathan et al. [7], based on Convolutional Neural Networks (CNN), proposed a method to classify and detect pests in the initial growth stage of corn, soybean, and wheat. Comparably, Nanni et al. [18] prepared an ensemble of CNNs consisting of AlexNet, GoogleNet, ShuffleNet, MobileNetv2, and DenseNet201. These studies show that an advantage of deep learning networks is that they do not require explicit background removal to train and classify images. However, they do demand a significant number of samples to converge accurately.

Based on the related work, we can note that computer-aided approaches that deal with crop pest detection consider the identification and classification of insects for this task. Nevertheless, we propose a different investigation strategy in this study. According to Carvalho et al. [19], the external-feeding fraction of insect damage has excellent potential for improving the understanding of ancient and extant herbivore communities. Thus, detecting sets of leaf damage types offer opportunities for assessing insect diversity or detecting changes in insect composition over climatic. Unfortunately, none of the abovementioned methods

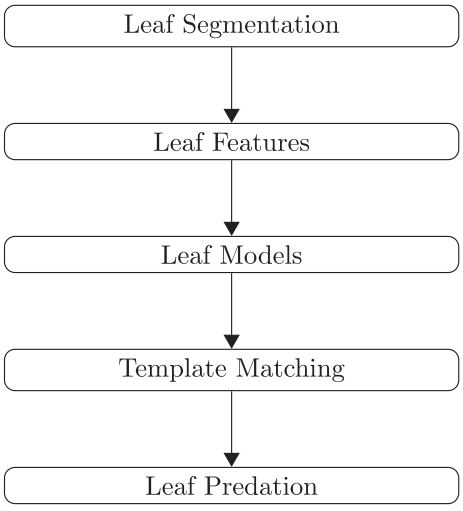


**Fig. 1.** Architecture components of the proposed method.

were developed to identify and isolate leaf damage, i.e., the bite signature caused by mandibular insects or insect-induced damage.

In this sense, in our proposal, leaf damage occurrences are identified and visually demarcated according to the regions in which they occur. Besides, the leaf damage lines formed from the herbivory are segmented to recognize bite patterns from their peculiarities. Therefore, we identified the presence of pests considering their harmful effects where the exacerbated leaf damage can inhibit the development of plants. From our perspective, plantation monitoring applications, especially real-time inspections, may benefit better from the approach we present because it is easier to find samples of leaf damage in crop fields than the insects that produced them. This study demonstrates that our method is invariant to scale, rotation, and image noise changes. Also, it requires few leaf samples to construct an image model for detecting and segmenting insect bite marks, with particular attention to damage in leaf border regions. We evaluated the proposed method using a challenging image database that includes different cultivars and variations of leaf samples (apple, blueberry, cherry, corn, grape, peach, pepper, potato, raspberry, soybean, strawberry, tomato).

## 3. Proposed method

The proposed method is divided into five parts. In the first, the images are segmented, and the image background is removed, preserving the leaf region. In the second, feature detectors are designed and used in the third step to build an image base with leaf models. In the fourth step, a similarity evaluator is formulated to select the appropriate image template for a damaged leaf image. Finally, the foliar damage regions are automatically detected and segmented in the last step. Fig. 1 provides an overview of the proposed method, described in the following subsections.

### 3.1. Leaf segmentation

The segmentation process consists of separating only the leaf region (area of interest) concerning the other regions of the image. In our study, each image $\mathbf{I_{RGB}}$ in the database is composed of two classes that describe the leaf or background regions. We use a median filter to assist this process with a kernel $\kappa$ of size $5 \times 5$. After applying this filter, we obtain new versions of the image channels, that are, $\mathbf{R}^*$, $\mathbf{G}^*$, and $\mathbf{B}^*$.

Then, we exceed the green color, $\mathbf{G}' = 2\mathbf{G}^* - \mathbf{R}^* - \mathbf{B}^*$, and the Otsu threshold method [20] is applied to obtain an optimum threshold value that separates the leaf pixels from the non-leaf pixels in $\mathbf{G}'$ and based on this step the background regions from $\mathbf{I_{RGB}}$ are removed. In this fashion, the original image is preserved without interference from the median filter applied to it and the approach of exceeding the green channel.

### 3.2. Leaf features

The feature extraction step is performed in two ways. In the first one, the leaf geometry is used to find a line representing the length of a leaf. While the second, the edge detector, is applied to find straight line-like structural descriptors.

In the initial step, the margin of the leaf is highlighted according to a binarization process that removes interior pixels to leave only the outline of the shapes. Then, the Mahalanobis distance is used to calculate the distances $d^2 \in \mathbf{D}^2$ between the vectors $v_s$ and $v_t \in \mathbf{V}$. The Mahalanobis distance is defined in Eq. (1),

$$d^2 = (v_s - v_t)C^{-1}(v_s - v_t)', \tag{1}$$

where $C$ is the covariance matrix. The vectors $v_s$ and $v_t$ represent the pairwise Cartesian coordinates $(x, y)$ of the margin of the leaf, for all $v_s$ and $v_t$ different from each other.

Then, the index of longest distance $d^*$ among all vectors in the leaf border is found using Eq. (2):

$$d^* = \arg\max(\mathbf{D}^2) \tag{2}$$

After that, the line connecting the two margin points ($A = v_s^{d^*} = (a_x, a_y)$ and $B = v_t^{d^*} = (b_x, b_y)$) represents the longest path, i.e., the length of the leaf which we refer to as the reference line.

In the second feature detection strategy, the Sobel edge detector is applied to the image $\mathbf{G}$, and the feature extraction process is performed to find straight line-like structural descriptors using the Hough transform [21]. Due to its ability to isolate features of a particular shape, the Hough transform technique is commonly used to detect regular curves such as lines, circles, and ellipses, image analysis, computer vision, and digital image processing [22].

### 3.3. Leaf models

Those two points that defined the length of the leaf, points $A$ and $B$, are used to adjust the leaf so that its apex (leaf tip) or base points upwards. First, the $\Delta$ between these two points is found using Eq. (3):

$$\Delta = \frac{a_y - b_y}{a_x - b_x}, \tag{3}$$

Then, the inverse tangent function of $\Delta$ is calculated, and the angle of rotation $\theta$ of the leaf relative to the image plane is found (Eq. (4)).

$$\theta = \arctan_{-90^\circ < \theta < +90^\circ}(\Delta) \tag{4}$$

Hence, the rotation angle $\theta$ is used to define a rotation matrix (Eq. (5)) and to apply a planar rotation to each point $\tilde{x} \in \mathbf{I_{RGB}}$, which results in a rotated image $\mathbf{I'_{RGB}}$.

$$R = \begin{bmatrix} \cos(\theta) & -\sin(\theta) \\ \sin(\theta) & \cos(\theta) \end{bmatrix} \tag{5}$$

After the rotation transformation, the leaf area is detected and surrounded by a rectangular bounding box. This delimited area is used to crop the image to contain only the leaf parts, discarding the leafless regions. Finally, the cropped image is resized to the same size as the original image, i.e., for size, $m$ by $n$, producing the $\mathbf{I''_{RGB}}$ image. Complementary, the rotation angles of the lines detected by the Hough transform relative to the image plane are also used to produce other transformed images.

### 3.4. Template matching

The template matching is performed by measuring the dissimilarity between damaged leaf area distributions with the prepared image

models. The earth mover's distance[1] (EMD) [23] is used, and the dissimilarities between them quantify the proximity between the damaged leaf to the image models. To perform this evaluation and in addition to the EMD[2], we propose a cost function that evaluates the correspondence between image pairs using their dissimilarities but also considering the non-overlapping areas between them.

The three terms of Eq. (6) represent the proposed cost function $c_o$.

$$c_o = \omega_1 + \omega_2 + \omega_3, \tag{6}$$

where

$$\omega_1 = EMD(\mathbf{I}_a, \mathbf{I}_b)$$

$$\omega_2 = \psi + \zeta + \phi$$

$$\omega_3 = \nu + \tau$$

and

$$F(\mathbf{I}_a, \mathbf{I}_b) = \frac{1}{nm}\sum_{i=1}^{n}\sum_{j=1}^{m}(p_{ij} \wedge q_{ij})$$

$$F_A(\mathbf{I}_a, \mathbf{I}_b) = \frac{1}{nm}\sum_{i=1}^{n}\sum_{j=1}^{m}(p_{ij} \vee q_{ij}) \wedge \neg(p_{ij} \wedge q_{ij})$$

$$\psi = F_A(\mathbf{I}_a, \mathbf{I}_b)$$

$$\zeta = F(\mathbf{I}_a, \neg\mathbf{I}_b)$$

$$\phi = F(\neg\mathbf{I}_a, \mathbf{I}_b)$$

$$\nu = F(\neg\mathbf{I}_a, \mathbf{w}_r)$$

$$\tau = F(\mathbf{I}_a, \neg\mathbf{w}_r)$$

let be $F(.,.)$ a function that averages the intersection of pixels that have true values in a binary image, for pixels $p \in \mathbf{I}_a$ and $q \in \mathbf{I}_b$. $F_A(.,.)$ is a function that calculates the area that is outside of the intersection between a damaged sample image and the input leaf; $\mathbf{I}_a$ and $\mathbf{I}_b$ are the image recovered by the method in the model and the input image of the leaf that the insect damages, respectively; $\zeta$ is the area that is in the input leaf but not in the damaged sample image; $\phi$ is the area that is in the damaged leaf sample but not in the input leaf; $\nu$ is the area that is in the leaf model but not in the input leaf; $\tau$ returns the area that is in the input leaf but not in the leaf model.

Then, with the cost resulting from the comparison performed, the leaf model with the smallest error is the chosen one, Eq. (7).

$$e = \arg\min(c_o), \tag{7}$$

where $e$ is the minimum error resulting from the cost function between the damaged leaf and all leaf models.

### 3.5. Leaf predation

To segment the insect predation areas, the margin of the damaged leaf **B** is detected, resulting in the logical image $\mathbf{B}'$. The damaged regions **S** are detected first based on the logical conjunction operation between $\mathbf{B}'$ and the retrieved image model **A** (Eq. (8)). Hence, **S** is updated by opening and dilating morphological operations. The opening operation is applied to remove spurious connected components with smaller pixels than $\beta$, and the dilation operation is applied to connect nearby components, according to a circular structural element of radius $r$. In the tests, $\beta$ and $r$ are set with 25 and 2, respectively.

$$\mathbf{S} = \mathbf{A} \wedge \mathbf{B}' \tag{8}$$

[1] It is also referred to as the Wasserstein distance and the Monge-Kantorovich problem.

[2] We use the code provided by Liu et al. [24] to calculate the earth mover's distance.

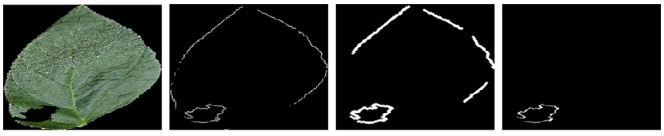

(a) (b) (c) (d)

**Fig. 2.** Detection of insect predation marks: (a) damaged leaf **B**, (b) predation areas **S** after Eq. (8), (c) **S** after opening and dilating operations, (d) **S** after eccentricity evaluation and erosion operation.

After applying the morphological operations, the eccentricity value of each of the remaining connected components is calculated to remove components that have structures similar to a straight line. It is performed to prevent the damaged leaf margins from being interpreted as predation areas when the damaged leaf is smaller than the retrieved image model. The eccentricity value is calculated according to Eq. (9)

$$E = \sqrt{1 - \left(\frac{b}{a}\right)^2}, \tag{9}$$

where $b$ is the length of the minor axis, and $a$ is the length of the major axis of an ellipse that contours a connected component in **S**.

The eccentricity value $E$ is between 0 and 1. When it is closer to 1, it is closer to being a line segment. After calculating the eccentricity, an evaluation is applied in which connected components smaller than a threshold $t$ are discarded. In the tests, we define $t$ as 0.98, which is a strict value so that only segments similar to lines are removed. Fig. 2 illustrates the process of detecting predation regions on a damaged leaf.

## 4. Material and methods

### 4.1. Image database

In the experiments, we used a public database[3] prepared by Hughes and Salathé [25]. In obtaining the samples, technicians sought a variety of lighting conditions, positioning, and foliar shape to prepare a diverse data set of leaf images obtained in various lighting conditions, including healthy and disease-affected leaves. From this database, we selected healthy leaf samples from 12 plants: apple, blueberry, cherry, corn, grape, peach, bell pepper, potato, raspberry, soybean, strawberry, and tomato. The size of the images is $256 \times 256$.

### 4.2. General setup

Each crop species in the database is divided into (1) data modeling and (2) test data. The first one is used to construct the leaf models, and the second one is used to validate the proposal. Tests are done individually for each leaf species, i.e., we do not mix samples from different classes. From each leaf species in the database, we select 20 leaf images to feed the data modeling group and 100 different images for the test data group. Thus, we worked with 140 images for the data modeling groups and 1.200 images for the test data groups. The validation is performed using the *K-fold* cross-validation strategy, which consists of splitting the available data into $K$ partitions, one for the data modeling group and the remaining $(K-1)$ for the test data group. In the experiments, $K$ is set to 5, so each test is run five times.

The experiments are divided into two parts. In the first one, we evaluate the behavior of our proposal in dealing with typical computer vision challenges such as scale-variation transformations, image rotation, and noise. Furthermore, we also investigated the impact of variations in defoliation levels when using the proposed method. In this part, which includes Sections 5.1–5.4, we consider only soybean leaves to prepare

[3] https://github.com/digitalepidemiologylab/plantvillage_deeplearning_paper_dataset.

the tests. In the second part of the experiment, another examination is performed to assess the capability of the proposed method in the detection and segmentation of insect predation on leaves of different crop species (apple, blueberry, cherry, corn, grape, peach, pepper, potato, raspberry, soybean, strawberry, tomato). Except for the test applied in Section 5.4, the defoliation level for the composition of the test group images is randomly selected from a range of 5 to 35%.

The accuracy of the proposed method is assessed with reference images made from healthy leaves that were automatically segmented using the image segmentation process (Section 3.1) and deformed to simulate leaf damage according to the synthetic defoliation strategy (Section 4.3). Thus, quantitative and visual inspections are obtained from different statistical measurements to compare our proposal outputs with the ground truth images.

The experiments were done in a notebook with Core i7-9750H (2.6GHz; 12MB Cache) and 16 GB RAM. As for the execution time, the entire construction process of the leaf models required 5.33 seconds for the 20 images in the data modeling group, which produced an average 48 leaf models, and 5.14 seconds to complete the process of evaluating and selecting a suitable model for each one of the features that were detected in the leaf test image. Thus, on average, each leaf in the test group has three features. The code was written using MATLAB and is available on-line[4].

### 4.3. Synthetic defoliation

We have prepared a synthetic defoliation strategy in which healthy leaves are subjected to a process capable of simulating insect predation. It consists of extracting bite signatures in real herbivory cases and preparing templates of foliar damage to promote different levels of leaf defoliation. The bite signature of two types of insects, *Spodoptera Frugiperda* and *Chrysodeixis Includens*, was extracted from injured leaves, resulting in some bite samples for each of the two insects. Although the defoliation examples are based on leaf chewers insects, multiple types of damage could be equally addressed according to the type of herbivore insects, such as bud feeders, hole feeders, skeletonizers, surface abrasion feeders, and sap-sucking. Thus, it can be addressed in future studies.

We developed a computer program that receives a healthy leaf as input and returns a damaged leaf and its level of defoliation. It uses four random variables to determine (1) the number of insect bites to use, (2) select one or more samples from the bite models, (3) apply a rotation transformation to the selected bite samples, (4) and resize the bite samples to a random size. Besides that, the defoliation level is an input parameter in which the desired defoliation level can be set from 1 to 99%.

### 4.4. Line segment assessment methodology

The evaluation of line segments (insect bite traces) considers a sequence of steps that includes image transformation operations and object matching. Initially, a morphological operation is applied on both detected bite segments and ground truth image segments to remove spurious pixels, followed by a dilation operation to connect small fragments of lines. Then, the pixels at the object's boundaries are removed, and the remaining pixels constitute the image's skeleton.

The objects are surrounded by bounding boxes whose function is to mark the area occupied by these objects. Each bounding box has an identifier used to track peer-to-peer matching operations. When an intersection between a bite segment and a segment in ground truth is perceived, the quality of the intersection is assessed using the IoA metric (presented in Section 4.5). If the result is positive, it is said that a True Positive (TP) was achieved. On the other hand, if there is no match for some bite segment, it is labeled as a False Positive (FP), and if there is no matching for some object in the ground truth, then it is considered a False Negative (FN). Fig. 3 illustrates all the steps used in the evaluation of bite segments.

Fig. 4 presents an illustration of how this evaluation is performed. In this example, two predation regions of an injured leaf were detected. Following the ground truth, only one was correctly identified. Thus, it can be observed that for one of the segmentation results, there is a correspondence (True Positive), while for another one, there is no matching (False Positive).

### 4.5. Evaluation metrics

To assess the output accuracy of our proposal, a quality factor known as $Q_{seg}$ [26] is used according to Eq. (10):

$$Q_{seg} = \frac{\sum_{i=1}^{m}\sum_{j=1}^{n} s_{i,j} \wedge r_{i,j}}{\sum_{i=1}^{m}\sum_{j=1}^{n} s_{i,j} \vee r_{i,j}}, \tag{10}$$

where $s_{i,j} \in \mathbf{S}$ is the retrieved leaf ($s_{i,j} = 1$) or background pixels ($s_{i,j} = 0$) and $r_{i,j} \in \mathbf{R}$ is the reference image, also in a binary format. The accuracy is based on logical operations, logical *and* ($\wedge$) and logical *or* ($\vee$), that compare the overlap between the reference image $\mathbf{R}$ and the retrieved image $\mathbf{S}$. $Q_{seg}$ varies in a range of values between 0.00 and 1.00 in which a value 1.00 represents a perfect consistency outcome between $\mathbf{R}$ and $\mathbf{S}$ images. $\mathbf{R}$ and $\mathbf{S}$ are binary images with size $m$ by $n$.

Furthermore, we compare the results between data distributions using the Kruskal-Wallis test [27], which is a non-parametric test that assesses whether the distribution functions are similar (null hypothesis $H_0$) or if there is any statistical difference between the functions under evaluation (alternative hypothesis $H_1$). A *p value* is returned, and it indicates which hypothesis will be rejected according to a limit of the significance level $\alpha$, in our case $\alpha = 0.05$. Also, a confidence interval is calculated according to Eq. (11).

$$P\left(\bar{x} - Z_s.\frac{\sigma}{\sqrt{n}} \leq \mu \leq \bar{x} + Z_s.\frac{\sigma}{\sqrt{n}}\right) = \gamma, \tag{11}$$

where $P$ refers to a probability function, $\bar{x}$, $\sigma$, and $n$ are the mean value, the standard deviation, and the size of the population sample, respectively. $Z_s$ is obtained from a *t-student* table regarding the confidence level $\gamma$, and $\mu$ is the unknown parameter of the average population expected to be in the confidence interval.

Besides, we prepared a modified version of the Intersection over Union (IoU) similarity index, and we call it Intersection over an Area (IoA). As conventional, in our version, the predicted and the ground truth segments are surrounded by bounding boxes, and these areas are used to measure their overlap. However, we do not use the union of these areas. In this sense, the IoA scores either complete segments or only some parts of them so that the difference between the measured values of these two cases does not have significant differences. This property is essential for our study because the contours that represent the insect predation segments can be discontinuous and interpreted as individual segments when, in fact, they are parts of the same bite segment. Therefore, predation segments labeled by the segmentation process are evaluated individually concerning the area they occupy.

The IoA similarity index is given by the intersection between the predicted predation segment and ground truth over the maximum area of predicted segments or the ground truth, Eq. (12).

$$IoA = \frac{\text{area}(\mathbf{Y}_i \wedge \mathbf{T}_j)}{\max(\text{area}(\mathbf{Y}_i), \text{area}(\mathbf{T}_j))} \tag{12}$$

where

$$\text{area}(x) = \sum_{i=1}^{m}\sum_{j=1}^{n} x_{i,j}$$

$\mathbf{Y_i}$ contains one of the $i$ predicted predation segment area compared with all $\mathbf{T}$ areas of predation from $j$ to the number of bites in the ground

[4] https://github.com/pixellab-ufg/leaf-analysis.

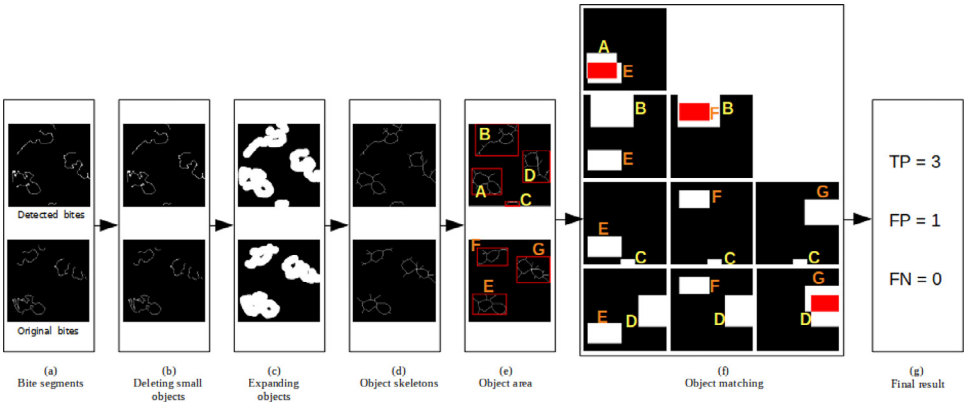


**Fig. 3.** Components of the bite segment assessment methodology.

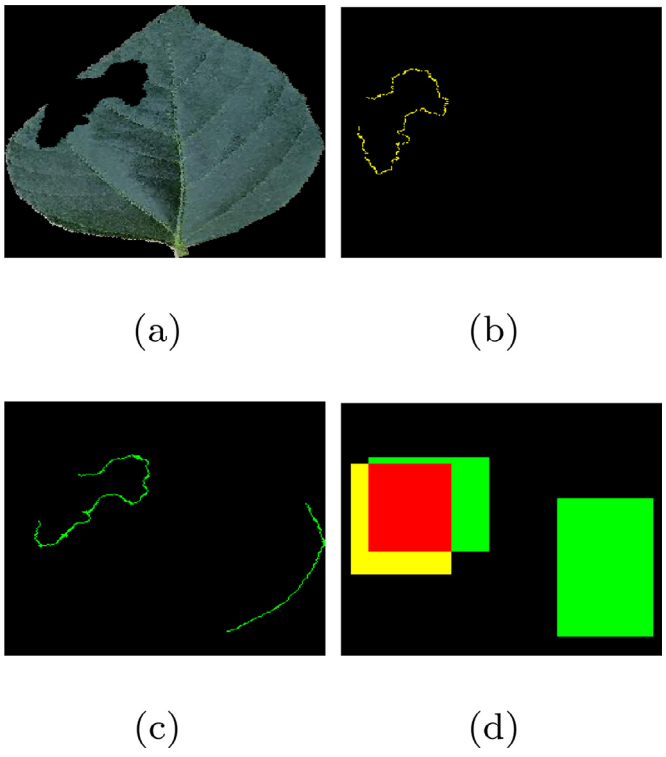


**Fig. 4.** Segmentation of insect predation marks and evaluation: (a) damaged leaf, (b) ground truth, (c) predation marks after bite detection, (d) ground truth area (yellow), predation areas (green) and the intersection between them (red). (For interpretation of the references to color in this figure legend, the reader is referred to the web version of this article.)

truth. Therefore, if the IoA of a bite segment is higher than 0.5, we define it as True Positive (TP). Otherwise, it is defined as False Positive (FP). Furthermore, those segments that do not match any predicted predation marks are defined as False Negative (FN).

From IoA, we used two statistical measures to evaluate the detection and segmentation of insect bite signatures. In Eq. (13) and Eq. 14, we describe the Precision and Recall measurements.

$$\text{Precision} = \frac{\text{TP}}{\text{TP} + \text{FP}} \tag{13}$$

$$\text{Recall} = \frac{\text{TP}}{\text{TP} + \text{FN}} \tag{14}$$

where TP stands for the number of segments correctly labeled as bite segments, FP represents the number of segments incorrectly labeled as a bite, and FN represents the number of bite segments that were not labeled as a bite. TP, FP, and FN are specified according to IoA scores.

## 5. Experimental design and results

### 5.1. Image scale variation

In this test, we simulate the variation in the positioning of cameras concerning their proximity and distance with the target objects. A factor $\lambda \in \{0.5, 0.6, 0.7, 0.8, 0.9, 1.0\}$ is used to resize the test data image group where a smaller value for $\lambda$ decreases the size of the images and a value of 1.0 means that the images are in their original size. Fig. 5(a) to (d) presents visual examples of this process.

Although the scale factor applied to the images significantly affects their resolution, the proposed method reaches similar results, even with this factor variation. For example, Fig. 6 shows that the median of the tests has similar results, which is confirmed by a Kruskal-Wallis $p = .95$. Therefore, even with scale variation, the proposal obtains satisfactory responses.

### 5.2. Image rotation transformation

Continuing with the camera positioning simulation, we investigate the effect of rotational transformations either by the camera or by positioning the target objects. A factor $\theta \in \{0, 90, 180, 270\}$ is applied to rotate the images of the test data group at different angles where $\theta = 0$ represents the images in their original positions. Fig. 5(e) to (h) presents visual examples of this process.

In Fig. 7, the median values of the test cases are consistent. In this sense, a Kruskal-Wallis $p = .33$ value indicates that the rotation transformation did not affect the distributions to the point of refuting the null hypothesis, which means that even with the application of this type of transformation, the results are stable.

### 5.3. Image noise variation

We also investigated the behavior of the proposed method in dealing with noisy images. We gradually add random salt & pepper noise with an density factor $\eta$, as in Eq. (15),

$$\eta \in \{0, 0.08, 0.16, 0.24, 0.32, 0.40\}, \tag{15}$$

to the images of the test data group in which for $\eta = 0$ no noise is applied, while for $\eta = 0.40$ noisy points are inserted in 40% of the input images.

When the addition of noise is applied, there is no significant change in the results concerning the images without noise, Fig. 8, confirmed by Kruskal-Wallis $p = .97$. However, we point out that the addition of noise has a minor influence on the segmentation process, causing leaf area loss or labeling non-leaf parts as the target object, as shown in Figs. 5(i) to (l).

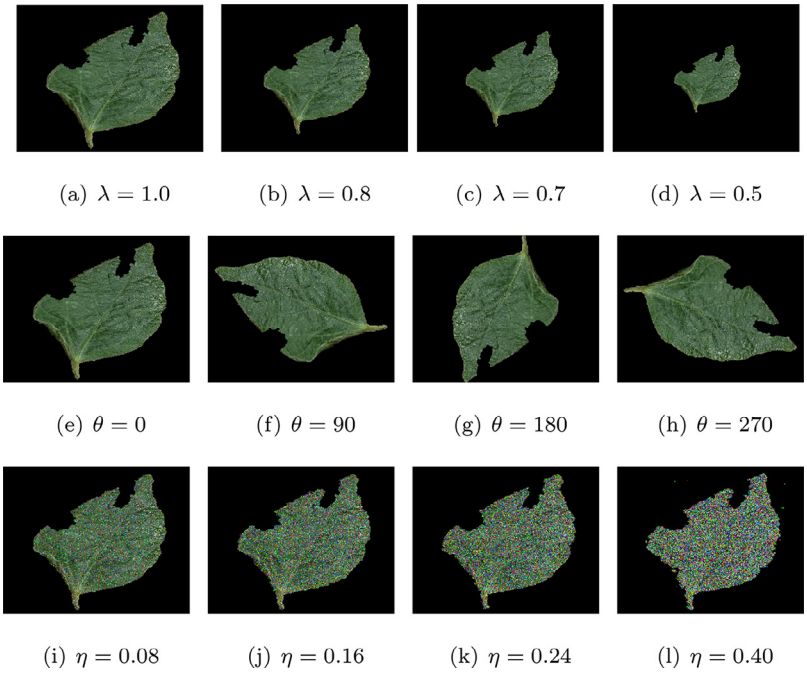


**Fig. 5.** Scale, rotation and noise variation. These samples are presented after the segmentation process and with 06.04% defoliation.

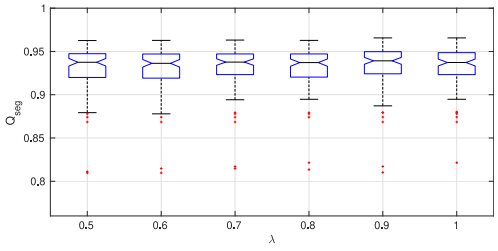


**Fig. 6.** Scale variation assessment.

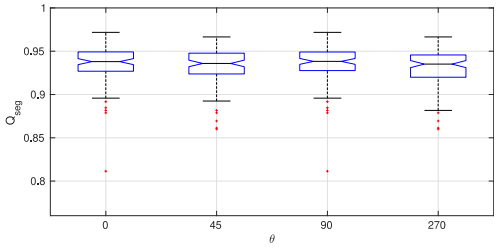


**Fig. 7.** Rotation transformation assessment.

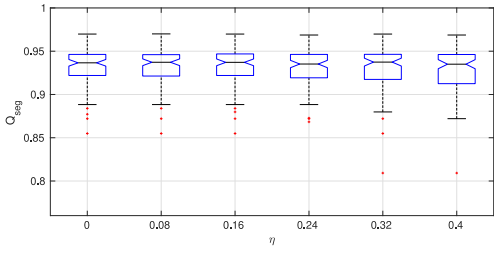


**Fig. 8.** Noise variation assessment.

### 5.4. Defoliation level range

In this test, we analyze the results of the proposed method when applying controlled changes in the percentage of leaf damage. Starting at 5%, we increase the defoliation level by 5% until reaching a maximum of 99% damage. Fig. 9 shows the mean, median, and standard deviation of the test cases. The results are best presented when the leaf damage varies from 1% to 35%. After that, the error increases, and the $Q_{seg}$ values decrease progressively. However, these results show us that our method provides suitable outputs even with a very high defoliation level, and the average $Q_{seg}$ is always higher than 0.79.

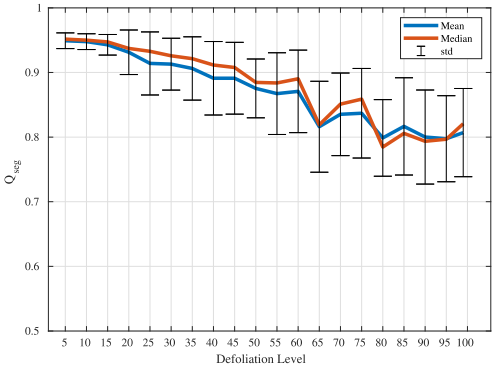


**Fig. 9.** Defoliation level assessment.

### 5.5. Detection and segmentation of insect predation

This experiment evaluates the proposed method for detecting and segmentation insect predation marks based on precision and recall measures. Fig. 10 shows the average statistical results for each crop species concerning the predation areas segmentation and, as it can be noted, among the five executions (*K-fold* cross-validation), there are only minor variations between the results with standard deviation values below 0.03.

Table 1 shows the general results obtained from the totality of the experimentation rounds with the average ($\mu$), standard deviation ($\sigma$), and minimum and maximum values from the five executions. Apple, blueberry, and cherry achieved over 86% precision and more than 80% recall. The characteristics of the database samples justify the high assertiveness of corn leaves (99% precision). As these leaves occupy the

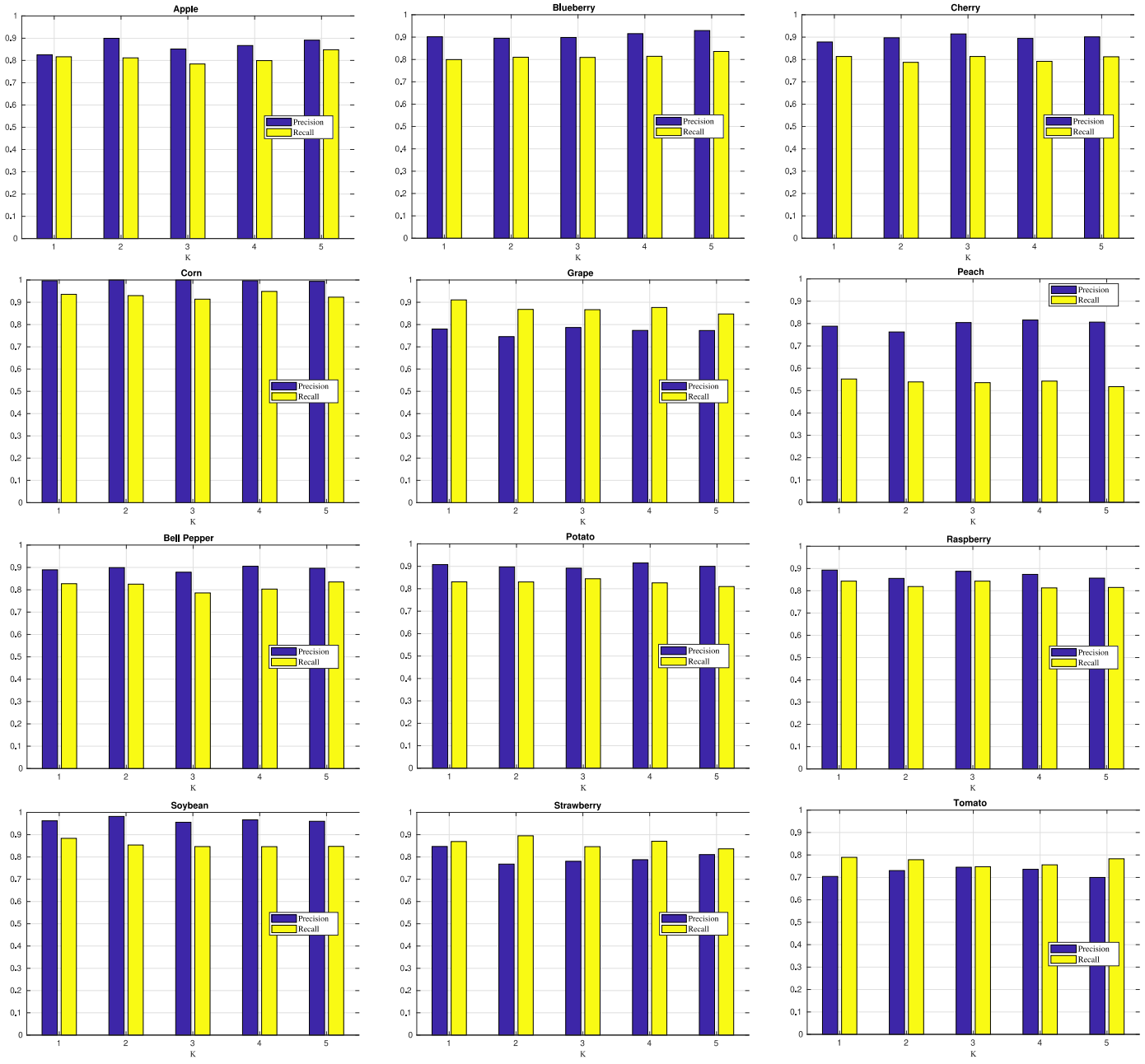


**Fig. 10.** Insect bite segmentation: average precision and recall. The x-axis represents the K-fold iteration number, while the y-axis represents the precision or recall outcomes.

**Table 1**
Precision and recall with the final scores between K-folds.

| | Precision | | | Recall | | |
|---|---|---|---|---|---|---|
| | $\mu$ / $\sigma$ | Min | Max | $\mu$ / $\sigma$ | Min | Max |
| Apple | 0.86 / 0.030 | 0.82 | 0.89 | 0.81 / 0.02 | 0.78 | 0.84 |
| Blueberry | 0.90 / 0.010 | 0.89 | 0.92 | 0.81 / 0.01 | 0.79 | 0.83 |
| Cherry | 0.89 / 0.010 | 0.87 | 0.91 | 0.80 / 0.01 | 0.78 | 0.81 |
| Corn | 0.99 / 0.002 | 0.99 | 0.99 | 0.93 / 0.01 | 0.91 | 0.94 |
| Grape | 0.77 / 0.010 | 0.74 | 0.78 | 0.87 / 0.02 | 0.84 | 0.91 |
| Peach | 0.79 / 0.020 | 0.76 | 0.81 | 0.53 / 0.01 | 0.51 | 0.55 |
| Bell Pepper | 0.89 / 0.010 | 0.87 | 0.90 | 0.81 / 0.02 | 0.78 | 0.83 |
| Potato | 0.90 / 0.009 | 0.89 | 0.91 | 0.82 / 0.01 | 0.81 | 0.84 |
| Raspberry | 0.87 / 0.010 | 0.85 | 0.89 | 0.82 / 0.01 | 0.81 | 0.84 |
| Soybean | 0.96 / 0.010 | 0.95 | 0.98 | 0.85 / 0.01 | 0.84 | 0.88 |
| Strawberry | 0.79 / 0.030 | 0.76 | 0.84 | 0.86 / 0.02 | 0.83 | 0.89 |
| Tomato | 0.72 / 0.020 | 0.70 | 0.74 | 0.77 / 0.01 | 0.74 | 0.78 |

entire image area, the template matching step can find suitable models for damaged leaves more accurately. It was expected behavior for the set of images of this class. Likewise, it was expected that the results for the peach leaf were not assertive due to the different shapes of the leaves and the shading effect on them. The results were inaccurate on the recall measure but surprising, with an average precision of 77%.

Unlike the other leaf classes, grape, strawberry, and tomato leaf samples obtained greater assertiveness in the recall measure than in precision, increasing at least five percentage points. As a result, grape and strawberry reached the second and third best recall value, only behind corn leaves. Besides, like most leaf classes, bell pepper, potato, and raspberry achieved recall values above 80% and precision values close to or equal to 90%. However, the main highlight is the soybean leaf, which reached 98% precision in some experimental tests.

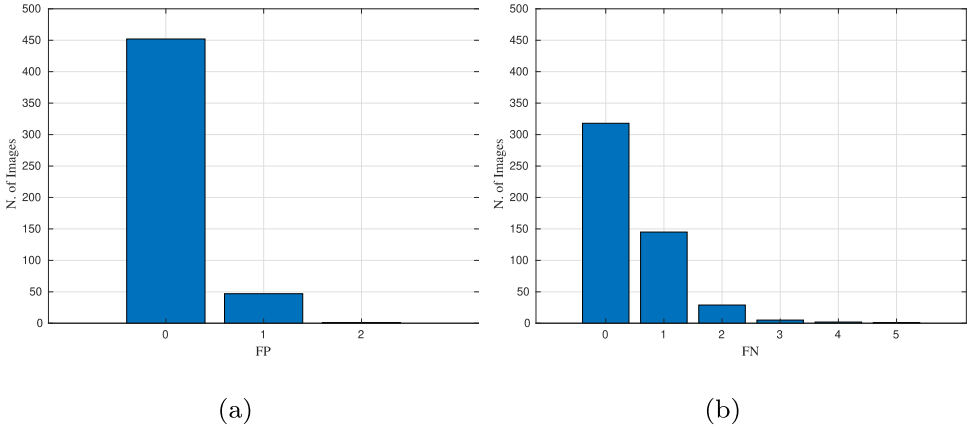


**Fig. 11.** Histogram of False Positive (FP) and False Negative (FN) obtained by the proposed method on soybean leaves. The x-axis represents the number of errors, while the y-axis represents the number of images in each range.

In addition, Fig. 11 shows histograms of the number of images by the total number of False Positive (FP) and False Negative (FN) segments across all runs. It is observed that most of the test images reported zero FP and FN entries; that is, 452 of the 500 test images (considering the five validation rounds) did not present FP segments, and for 318 images, there were no FN entries. Thus, there are more segments labeled as FN than FP. However, the maximum number of false-positive entries in a leaf sample was 2, while 5 false-negative entries were observed in just one image. Although these histograms were prepared with the results of the soybean leaf, for the other types of leaf, this behavior pattern is quite similar.

The interpretation of False Positive (FP) and False Negative (FN) consists of the attention given to the number of segments wrongly identified or ignored. False positives occur when bite segments are detected but do not match the actual bite segments. On the other hand, when actual bite segments are not detected, the method fails to identify the segments correctly, and the number of false negatives increases. Therefore, it is essential to balance these measures to correctly recognize bite segments, preventing them from being lost or misidentified. As can be seen, the proposed method has good assertiveness indices to address this issue, presenting accurate results in the detection and segmentation of insect bites.

## 6. Discussion of the results

Computer vision-based systems have proven essential in several areas, including agricultural applications in which management processes are improved, inspection activities are optimized, and decisions are made considering statistical data collected by sensors. Foliar loss caused by insect predation is an example where computer vision solutions are being applied to support proactive and reactive strategies in managing crop fields. On the other hand, there are some challenges related to the computer vision area that reduce the assertiveness of automated systems. In this sense, we proposed a new method for detecting leaf damage caused by insects. Also, we provided several tests using a complex database whose content includes entries of different plant species, leaf samples under different lighting conditions, leaves positioned at different angles, and leaf format with wide variation.

To design the experiments, we developed a defoliation method that applies synthetic damage to the edges of the leaves. We controlled the defoliation percentage, and we configured it so that the damage was applied randomly in the range of 5 to 35% in each leaf of the test group. The proposed method was demonstrated to be effective in the presence of noise and image transformations as scale and rotation. Thus, the positioning of the camera, or the leaf, during the image acquisition process does not need to follow a strict control scheme (Sections 5.1, 5.2 and 5.3). Besides, our method showed more accurate results for leaves with up to 35% damage, which is consistent with actual assessments, as damage above that percentage would, in many cases, imply an irreparable loss (Section 5.4).

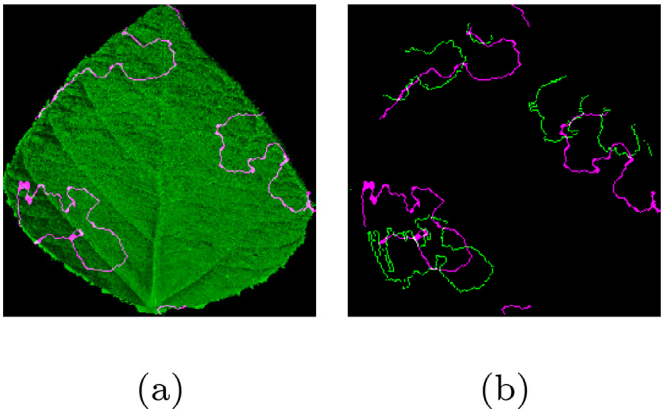


**Fig. 12.** Bites segments and grount truth: (a) Bite segments superimposed on the image model, (b) Misalignment between bite segments (magenta) and gruth truth (green). (For interpretation of the references to color in this figure legend, the reader is referred to the web version of this article.)

Furthermore, we have shown that the proposed method accurately identifies insect predation areas regardless of the plant species affected (Section 5.5). Statistical measures were consulted, and precision above 90% was achieved in the blueberry, corn, potato, and soybean leaves, and, except for tomato and peach, all other leaf classes, such as apple, cherry, grape, bell pepper, raspberry, and strawberry, achieved a recall higher than 80%. In this assessment, we modified the traditional metric IoU to allow a fair evaluation. We did that because the bite segments could contain discontinuities, and when compared to the ground truth, the covered area (i.e., the area that consists of the union between them) could be significantly larger than the intersection area and vice versa. Furthermore, there is no guarantee that the bite segments will align with the ground truth images, making it difficult to perform a direct overlay comparison. These facts greatly influenced the results, increasing the false-positive or false-negative rate, even when we visually observed a significant intersection between the parts evaluated. Fig. 12(a) shows an example of the overlay of insect bite segments on their corresponding image model. It is noticed that the representation of the segments under the image is almost perfect, but when compared to the ground truth, there is a disarrangement between the bite segments (Fig. 12(b)). The assessment methodology presented in Section 4.4 addresses issues of this type.

Table 2 compares the proposed method with some related works. The first five studies addressed classification algorithms for different insect species. In three of these studies, the regions occupied by them were highlighted, making it possible to visually verify the location of

**Table 2**
Characteristis of our proposal and related work.

| Research Work | Insect Classification | Location of Insect Occurrence | Insect Damage Detection | Method | Dataset |
|---|---|---|---|---|---|
| [10] | Yes | No | No | ML | PD |
| [15] | Yes | Yes | No | ML | LD, PD |
| [17] | Yes | Yes | No | ML | LD |
| [7] | Yes | Yes | No | ML | PD |
| [18] | Yes | No | No | ML | PD |
| [28] | No | No | Yes | ML | LD |
| [29] | No | No | Yes | ML | LD, PD |
| [30] | No | No | Yes | ML | PD |
| [31] | No | No | Yes | PR | PD |
| **Our** | No | Yes | Yes | PR | PD |

**LD**: Local Dataset, **PD**: Public Dataset, **ML**: Machine Learning, **PR** Pattern Recognition.

insects in the scenarios investigated by the authors. However, none of them pointed to regions of insect damage. On the other hand, in the works of Machado et al. [28], da Silva et al. [29], and Silva et al. [30], methods were proposed to estimate leaf loss, and even without the detection and classification of insects, it is possible to infer their presence when considering the percentage of loss. Our proposal offers a balance between these works where the places of occurrence of insects can be verified as well as the regions of damage caused by them. In addition, it is observed that, except for our work and another one published by us Vieira et al. [31], the other works use machine learning to design their methods. Also, most research uses public databases.

In terms of method limitations, we point out that the data modeling group can negatively influence the assertiveness of the proposed method if the models are significantly different from the defoliated images. For example, insect predation marks may be lost if the leaves used to build the models are smaller than the leaves under test. On the other hand, if the model's size is larger than the leaves under analysis, there is still a chance that insect predation segments can be preserved. Such limitations can be overcome if the image database has more homogeneous characteristics in the leaf samples. Furthermore, stems, branches, and more than one leaf per photo could interfere with the interpretation and decrease assertiveness, as can occur in images recorded directly from

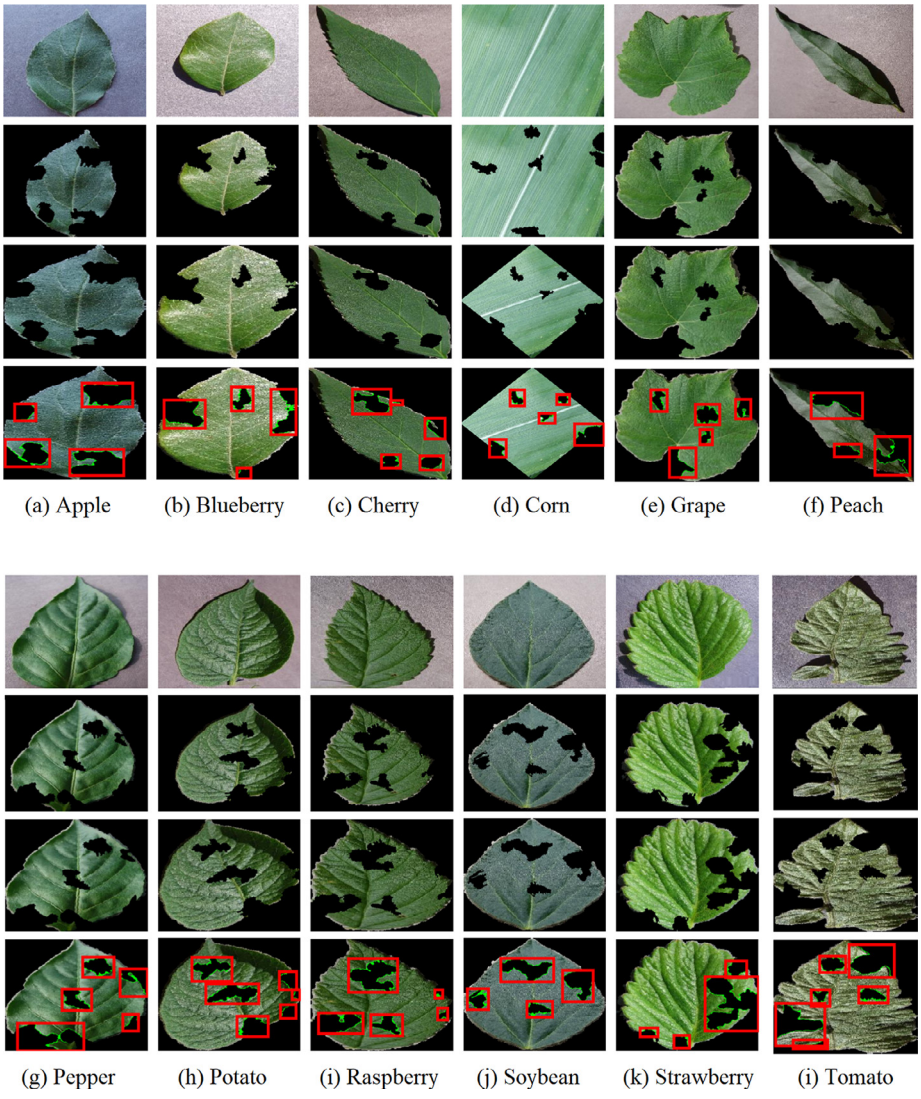


**Fig. 13.** Detection of insect predation regions and segmentation of bite marks on injured leaves. The first rows show the original images, the second rows present the images after segmentation and defoliation, the third rows show the leaves after image adjustment, and the fourth rows present the final result of the detection and segmentation of the bites segments.

live plants. Despite the limitations presented, the results are promising, as shown in Fig. 13 where a sample of each crop species is presented with visible results of bite segmentation achieved after applying the proposed method.

## 7. Conclusions

This paper proposed an automatic method for detecting injured leaf areas caused by insect predation. We validate the proposal's performance using a complex database whose content encompasses several types of cultivation and leaf samples with different morphological structures. We show that the method effectively highlights the damaged regions and segments the bite contours of predatory insects. A precision of over 90% was achieved for blueberry, corn, potato, and soybean crops. Also, a recall of more than 86% for grape and strawberry. We conclude that this work opens up new possibilities for leaf analysis, reduces human effort in visualizing the occurrence of pests, and encourages the classification of insects based on bite patterns.

Future research includes expanding the study to evaluate additional data sets and applying different insect species to generate leaf damage. Also, different optimization parameters can be experimented with, and other leaf deformation models. Besides, the proposed method can be used as an initial step in classifying insects through their bite properties.

## Declaration of Competing Interest

We wish to confirm that there are no known conflicts of interest associated with this publication and there has been no significant financial support for this work that could have influenced its outcome.

We confirm that the manuscript has been read and approved by all named authors and that there are no other persons who satisfied the criteria for authorship but are not listed. We further confirm that the order of authors listed in the manuscript has been approved by all of us.

We confirm that we have given due consideration to the protection of intellectual property associated with this work and that there are no impediments to publication, including the timing of publication, with respect to intellectual property. In so doing we confirm that we have followed the regulations of our institutions concerning intellectual property.

We understand that the Corresponding Author is the sole contact for the Editorial process (including Editorial Manager and direct communications with the office). He is responsible for communicating with the other authors about progress, submissions of revisions and final approval of proofs. We confirm that we have provided a current, correct email address which is accessible by the Corresponding Author.

Finally, we declare that the manuscript "Automatic detection of insect predation through the segmentation of damaged leaves" is original and it is not being considered by any other publishing elsewhere. We have no conflicts of interest to disclose.

## Acknowledgments

The authors would like to thank the Federal Institute Goiano for supporting this research and thank the anonymous reviewers for their constructive comments to improve the paper. Moreover, authors would like to thank CAPES (Coordenação de Aperfeiçoamento de Pessoal de Nível Superior – Brazil) [CAPES Finance Code #001] for the financial support.

## References

[1] USDA, 2020a. World agricultural production. Available at: https://downloads.usda.library.cornell.edu/usda-esmis/files/5q47rn72z/ft849d88n/q811m8874/production.pdf Accessed: 2020-12-08.
[2] USDA, 2020b. Grain: world markets and trade. Available at: https://apps.fas.usda.gov/psdonline/circulars/2020/11/grain.pdfAccessed: 2020-12-08.
[3] USDA, 2020c. Sugar: world markets and trade. Available at: https://apps.fas.usda.gov/psdonline/circulars/2020/10/sugar.pdf Accessed: 2020-12-08.
[4] USDA, 2020d. Fresh apples, grapes, and pears: world markets and trade. Available at: https://apps.fas.usda.gov/psdonline/circulars/2020/10/fruit.pdf Accessed: 2020-12-08.
[5] USDA, 2020e. Fresh peaches and cherries: world markets and trade. Available at: https://apps.fas.usda.gov/psdonline/circulars/2020/11/stonefruit.pdf Accessed: 2020-12-08.
[6] D. Pivoto, P.D. Waquil, E. Talamini, C.P.S. Finocchio, V.F.D. Corte, G. de Vargas Mores, Scientific development of smart farming technologies and their application in brazil, Inform. Process. Agricu. 5 (1) (2018) 21–32, doi:10.1016/j.inpa.2017.12.002.
[7] T. Kasinathan, D. Singaraju, S.R. Uyyala, Insect classification and detection in field crops using modern machine learning techniques, Inform. Process. Agricu. (2020), doi:10.1016/j.inpa.2020.09.006.
[8] C.-Y. Lu, D.J. Arcega Rustia, T.-T. Lin, Generative adversarial network based image augmentation for insect pest classification enhancement, IFAC-PapersOnLine 52 (30) (2019) 1–5, doi:10.1016/j.ifacol.2019.12.406. 6th IFAC Conference on Sensing, Control and Automation Technologies for Agriculture AGRICONTROL 2019.
[9] K. Thenmozhi, U. Srinivasulu Reddy, Crop pest classification based on deep convolutional neural network and transfer learning, Comput. Electron. Agricu. 164 (2019) 104906, doi:10.1016/j.compag.2019.104906.
[10] J. Wang, C. Lin, L. Ji, A. Liang, A new automatic identification system of insect images at the order level, Knowl.-Based Syst. 33 (2012) 102–110, doi:10.1016/j.knosys.2012.03.014.
[11] C. Wen, D. Guyer, Image-based orchard insect automated identification and classification method, Comput. Electron. Agricu.e 89 (2012) 110–115, doi:10.1016/j.compag.2012.08.008.
[12] C. Xie, J. Zhang, R. Li, J. Li, P. Hong, J. Xia, P. Chen, Automatic classification for field crop insects via multiple-task sparse representation and multiple-kernel learning, Comput. Electron. Agricu. 119 (2015) 123–132, doi:10.1016/j.compag.2015.10.015.
[13] H.-P. Yang, C.-S. Ma, H. Wen, Q.-B. Zhan, X.-L. Wang, A tool for developing an automatic insect identification system based on wing outlines, Sci. Rep. 5 (1) (2015) 12786, doi:10.1038/srep12786.
[14] K. Thenmozhi, U.S. Reddy, Image processing techniques for insect shape detection in field crops, in: 2017 International Conference on Inventive Computing and Informatics (ICICI), IEEE, Coimbatore, 2017, pp. 699–704, doi:10.1109/ICICI.2017.8365226.
[15] L. Deng, Y. Wang, Z. Han, R. Yu, Research on insect pest image detection and recognition based on bio-inspired methods, Biosyst. Eng. 169 (2018) 139–148, doi:10.1016/j.biosystemseng.2018.02.008.
[16] X. Cheng, Y. Zhang, Y. Chen, Y. Wu, Y. Yue, Pest identification via deep residual learning in complex background, Comput. Electron. Agricu. 141 (2017) 351–356, doi:10.1016/j.compag.2017.08.005.
[17] Y. Shen, H. Zhou, J. Li, F. Jian, D.S. Jayas, Detection of stored-grain insects using deep learning, Comput. Electron. Agricu. 145 (2018) 319–325, doi:10.1016/j.compag.2017.11.039.
[18] L. Nanni, G. Maguolo, F. Pancino, Insect pest image detection and recognition based on bio-inspired methods, Ecolog. inform. 57 (2020) 101089, doi:10.1016/j.ecoinf.2020.101089.
[19] M.R. Carvalho, P. Wilf, H. Barrios, D.M. Windsor, E.D. Currano, C.C. Labandeira, C.A. Jaramillo, Insect leaf-chewing damage tracks herbivore richness in modern and ancient forests, PloS one 9 (5) (2014) e94950.
[20] N. Otsu, A threshold selection method from gray-level histograms, IEEE Transact. Syst. Man Cybernet. 9 (1) (1979) 62–66.
[21] R.O. Duda, P.E. Hart, Use of the hough transformation to detect lines and curves in pictures, Commun. ACM 15 (1) (1972) 11–15.
[22] R.C. Gonzalez, R.E. Woods, Digital Image Processing, Prentice Hall, Upper Saddle River, N.J., 2008.
[23] Y. Rubner, C. Tomasi, L.J. Guibas, The earth mover's distance as a metric for image retrieval, Int. J. Comput. Visi. 40 (2) (2000) 99–121.
[24] J. Liu, W. Yin, W. Li, Y.T. Chow, Multilevel optimal transport: a fast approximation of wasserstein-1 distances, arXiv preprint arXiv:1810.00118 (2018).
[25] D.P. Hughes, M. Salathé, An open access repository of images on plant health to enable the development of mobile disease diagnostics through machine learning and crowdsourcing, ArXiv abs/1511.08060 (2015).
[26] P. Sadeghi-Tehran, N. Virlet, K. Sabermanesh, M.J. Hawkesford, Multi-feature machine learning model for automatic segmentation of green fractional vegetation cover for high-throughput field phenotyping, Plant Method. 13 (1) (2017) 103.
[27] W.H. Kruskal, W.A. Wallis, Use of ranks in one-criterion variance analysis, J. Am. Stati. Assoc. 47 (260) (1952) 583–621.
[28] B.B. Machado, J.P. Orue, M.S. Arruda, C.V. Santos, D.S. Sarath, W.N. Goncalves, G.G. Silva, H. Pistori, A.R. Roel, J.F. Rodrigues-Jr, Bioleaf: a professional mobile application to measure foliar damage caused by insect herbivory, Comput. Electron. Agricu. 129 (2016) 44–55.
[29] L.A. da Silva, P.O. Bressan, D.N. Gonçalves, D.M. Freitas, B.B. Machado, W.N. Gonçalves, Estimating soybean leaf defoliation using convolutional neural networks and synthetic images, Comput. Electron. Agricu. 156 (2019) 360–368, doi:10.1016/j.compag.2018.11.040.
[30] M. Silva, S. Ribeiro, A. Bianchi, R. Oliveira, An improved deep learning application for leaf shape reconstruction and damage estimation, in: Proceedings of the 23rd International Conference on Enterprise Information Systems - Volume 1: ICEIS, INSTICC, SciTePress, 2021, pp. 484–495, doi:10.5220/0010444204840495.
[31] G. Vieira, N. Sousa, B. Rocha, A.U. Fonseca, F. Soares, A method for the detection and reconstruction of foliar damage caused by predatory insects, in: 2021 IEEE 45th Annual Computers, Software, and Applications Conference (COMPSAC), 2021, pp. 1502–1507, doi:10.1109/COMPSAC51774.2021.00223.